

## TECHNICAL PAPER

## HRPD AND TEM STUDY OF P/M 58Fe17Cr25Ni AUSTENITIC STAINLESS STEEL SYNTHESIZED BY SPARK PLASMA SINTERING

Salim Mustofa<sup>1</sup>, Mohammad Dani<sup>2</sup>, Parikin<sup>2</sup>, Toto Sudiro<sup>3</sup>, Bambang Hermanto<sup>3</sup>, Damar Rastri Adhika<sup>4,5</sup>, Andon Insani<sup>6</sup>, Syahbuddin<sup>7</sup>, Takanori Hino<sup>8</sup>, Ching An Huang<sup>9</sup>

<sup>1</sup>Dir. of Strengthening & Partnership of Infrastructure Res. & Innov., DIRI BRIN, Raya Jakarta Bogor KM 47 Cibinong, West Java 16915, Indonesia.

<sup>2</sup>Research Center for Nuclear Reactor Tech., OR TN BRIN, Puspiptek Serpong, South Tangerang, Banten 15314, Indonesia.

<sup>3</sup>Research Center for Advanced Material, OR NM BRIN, Puspiptek Serpong, South Tangerang, Banten 15314, Indonesia.

<sup>4</sup>Research Center for Nanosciences and Nanotechnology, Bandung Institute of Tech., Jl. Ganesha 10, Bandung, West Java 40132, Indonesia.

<sup>5</sup>Adv. Functional Mat. Res. Group, Fac. of Industrial Tech., Bandung Institute of Tech., Jl. Ganesha 10, Bandung, West Java 40132, Indonesia.

<sup>6</sup>Research Center for Radiation Detection Tech. & Nuclear Analysis, OR TN BRIN, Puspiptek Serpong, South Tangerang, Banten 15314, Indonesia.

<sup>7</sup>Dept. of Mechanical Eng., Fac. of Eng., Universitas Pancasila, SrengsengSawah, Jagakarsa, South Jakarta, DKI 12640, Indonesia

<sup>8</sup>Dept. of Material Engineering, Niihama National College of Technology, Niihama, Ehime, Japan.

<sup>9</sup>Dept. of Mechanical Engineering, Chang Gung University, Taoyuan, Taiwan.

\*Corresponding author: [sali002@brin.go.id](mailto:sali002@brin.go.id), telp: +62 811 8612 392, B.J. Habibie Jalan M.H. Thamrin Nomor 8, Central Jakarta, DKI 10340, Indonesia

Received: 03.07.2022

Accepted: 06.10.2022

## ABSTRACT

In this study, 58Fe17Cr25Ni austenite stainless steel has been fabricated using metal powder through sintering with a spark plasma at temperatures of 900 and 950°C for a time of 5 minutes. High purity Fe, Ni and Cr powders were used as materials for this steel. Before sintering, the powder was mixed in a milling equipment which was processed for 5 hours, then it formed into a coin by pressing it under a load of 25 tons. The microstructure and phases in the 58Fe17Cr25Ni austenite stainless steel were characterized through an optical microscope, a scanning electron microscope, a transmission electron microscope, with the last two devices equipped with an energy dispersion spectrometer. High resolution powder neutron diffractometer was also used for identifying the crystal structure in the 58Fe17Cr25Ni austenitic stainless steel. The sintering process at temperatures of 900°C and 950°C generally forms microstructure having matrix of equiaxed austenite grains, with a crystal structure of face-centered cubic which included in the Fm3m space group. Some particles with high Cr content,  $\alpha$ -Cr, are distributed in all austenite grains. In more detailed observations, the austenite grains seen in the 58Fe17Cr25Ni austenitic stainless steel sintered at 900°C are twin grains. Dislocations, slip planes and bands are also existed in those grains. These defects are expected to decrease with increasing sintering temperatures up to 950°C. This change was followed by the appearance of air bubbles and sub-grains as the dominant sub-structures in the 58Fe17Cr25Ni austenitic stainless steel sintered at 950°C.

**Keywords:** SPS; 58Fe17Cr25Ni ASS; SEM; TEM; HRPD

## INTRODUCTION

One of the many stainless steels that have long been used as a component of jet engines, power plants including nuclear power plants is austenitic stainless steel [McGuire2008, Zinkle2009]. Through its austenite grains and other intermetallic compounds, this steel has high strength, corrosion resistance [Irena Vlčková 2016, Sakata, K. 2016] and creep resistance so that it can withstand high temperature environments. The properties are strongly related to the contents of the main

elements such as Ni and Cr, in addition to other additional elements such as Mo, Mn, Ti, Nb, V, Cu, Al, Si, C and N for specific functions [Ducki2015, Plaut2007, Sourmail2001] in stainless steel austenitic. Generally, steel consists of wrought and cast products. Another is a product of powder metallurgy. Although they offer better mechanical properties and greater homogeneity, austenitic stainless steel formed by powder metallurgy are rarely found in the commercial market. Some recent researchers have been carried out using powder metallurgy method to synthesis austenitic stainless steel [Naci2013,

Akhtar2011, Keller2016, Choi2015]. In addition, the latest powder metallurgy technique with spark plasma sintering offers better results such as high density, ultra-fine structure and short sintering time compared to conventional techniques [Cavaliere2019]. By applying conventional sintering, Akhtar et.al [Akhtar 2011] investigated the effects of sintering temperatures and the MoSi<sub>2</sub> content up to 10.0% on the evolution of the microstructure and mechanical properties of 316L stainless steel. Using a combination technique of ball-milling and plasma sintering, fabrication of 316L ASS powder [Keller2016] has been studied in relation to the parameter condition of spark plasma sintering. Another technique has also been developed by a study [Choi2015] to produce product of powder metallurgy. It has successfully developed a powder injection mold for making 316L stainless steel micro-nanopowders. Most works are related to 316L austenitic stainless steel. Few are interested in studying the powder metallurgy of austenitic stainless steel for nuclear power plant components such as A286 austenitic stainless steel. In addition, most our works [M. Dani2019, S. Mustofa2019] which have been developed is concerned to 17Cr25Ni austenite stainless steel which has the chemical composition close to of A286 ASS composition. Thus, this study develops a powder alloy of 58wt% Fe, 17wt% Cr and 25wt% Ni by using arc plasma sintering. The sintering temperatures were set at temperatures of 900 and 950°C with a duration of 5 minutes.

Some characterization equipment's such an optical microscope (OM), a Scanning Electron Microscopy (SEM) and a transmission electron microscope (TEM), both completed by energy dispersed spectrometer (EDS) were used for identifying defects, phases and crystal structures formed in the microstructure of 58Fe17Cr25Ni austenitic stainless steel after sintering by a spark plasma at 900 and 950°C. Additionally, a high resolution powder neutron diffractometer (HRPD) also were used for characterizing the austenitic stainless steel. Therefore, in this study, details of the microstructure including defects such as dislocations, slip planes, slip bands, air bubbles, particles and sub grains formed in the austenite grains after sintering at different temperatures of 900 and 950 C are also discussed in this study. Although the selected temperatures are slightly lower for the sintering temperature range for stainless steels, they are thought to still be able to conduct the diffusion process that is characteristic of the sintering process. Moreover, most sintering using SPS can be done at those temperatures.

## MATERIAL AND METHODS

### Material and characterization

High purity metal powders (99,99%) of Fe, Cr, and Ni are used to fabricate 58Fe17Cr25Ni austenitic stainless steel (ASS) through processes of spark plasma sintering (SPS). Nominal each element in weight% is 58.0, 17.0 and 25.0%. For whole discussion in this study, all element contents are mentioned by weight %. The three powders were mixed using a milling device for 5 hours and compacted under 30 MPa. The compaction resulted in a coin with a diameter of 15 mm and a thickness of 2.5 mm. The coin was sintered by SPS, Fuji-625 (Fuji Industrial Co., Ltd), at temperatures of 900 and 950°C for time of 5 minutes.

Examination crystal structure of grains in the 58Fe17Cr25Ni ASS was performed by a HRPD in the Siwabessy Nuclear Reactor Puspitpek Serpong, Indonesia. To reveal the microstructure of 58Fe17Cr25Ni ASS, sample was prepared through a standard metallurgical process that includes grinding on SiC sandpapers from a rough grid size of 200 to fine grid size of

5000. Then it was polished with a paste containing diamond particles of a maximum size of 1 μm and then etched into a Kalling reagent solution for a time of 15 seconds. The microstructure of the 58Fe17Cr25Ni ASS was observed using an optical microscope (OM), a scanning electron microscope (SEM) of JSM-7600F (Jeol Ltd., Tokyo, Japan) that was operated at a voltage of 20 kV and a transmission electron microscope (TEM) of Hitachi H-9500 operated at a voltage of 300 kV. The last two devices are completed by energy dispersive spectrometers (EDS) for determining the composition of phases formed in the ASS. In addition, a micro-sampling method was performed on the Hitachi FB-2200 focused ion beam (FIB) at an operating voltage of 40 kV for preparation of TEM samples.

The variation in time on temperatures and strokes during sintering at temperatures of 900 and 950 °C for 5 minutes is presented in **Fig. 1**. Two red curves relate to variations in sintering temperature. The other two blue colours are stroke variations. Initially, the sintering temperature has a constant value of around 580°C for 300 seconds, rising sharply to 650°C and the temperature curves decrease but remains at a high rate of up to 900°C for 200 seconds. After that, the sintering temperature rate decreases to temperatures of 900 and 950°C and respectively hold for about 600 seconds and then drop to about 580°C. As seen in stroke curves during sintering at temperatures of 900 and 950°C, initially both press distances have same paths to about 2.0 mm for 300 seconds and then the strokes increase instantly and at high rate to 2.6 mm for sintering at temperatures of 950°C and 2.8 mm for sintering at 900°C, each in 500 sec. Movement of both strokes back to constant value (2.6 mm) for up to 1300 s.

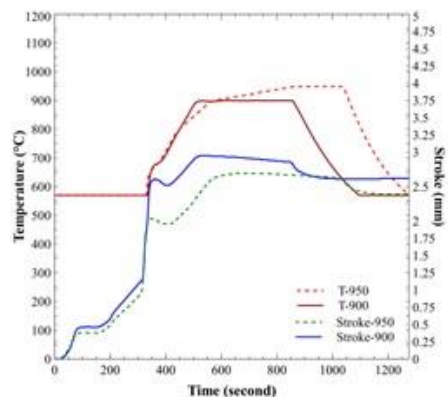


**Fig. 1** Graphics of sintering temperatures, strokes versus times for 58Fe17Cr25Ni austenitic stainless steels at temperatures of 900 and 950°C for time of 5 minutes.

## RESULTS AND DISCUSSION

### Matrix of 58Fe17Cr25Ni ASS

As seen in **Fig. 2**, some sharp peaks release in the HRPD after sintering either at temperatures of 900 or 950°C for 5 minutes. In both the diffraction patterns, those peaks are noticed to have relation to (111), (200), (220), (311) and (222) planes that might be available for a crystal structure of face centered-cubic (FCC). Such a crystal structure in stainless steels is known to have an austenite phase that is included in the Fm3m space

group. Moreover, the peaks found in the HRPD are very sharp, indicating that the ASS contains perfect crystalline.

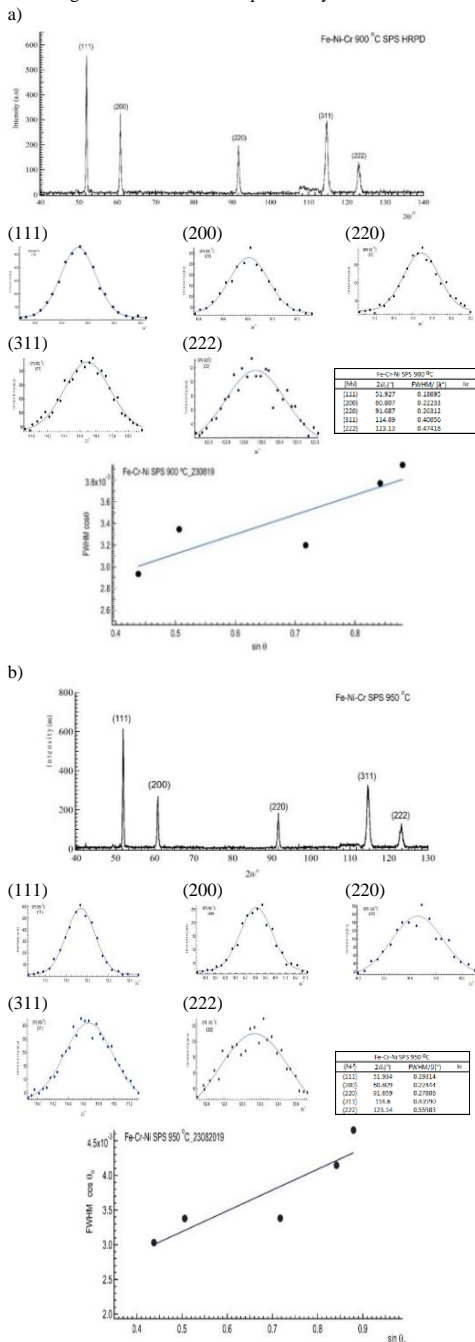


Fig. 2 HRPD Diffraction patterns of 58Fe17Cr25Ni ASS sintered by SPS at temperatures of a) 900 and b) 950°C for 5 minutes.

The lattice parameters of the diffraction pattern that were successfully calculated by the Rietveld method, as presented in Table 1, are  $a = 3.593 \text{ \AA}$  and  $a = 3.592 \text{ \AA}$  after sintering by SPS at temperatures of 900 and 950°C respectively. Using another method such as the x-ray diffraction pattern, the lattice parameters were measured by same method are  $a = 3.5877 \text{ \AA}$  and  $a = 3.5876 \text{ \AA}$  after sintering at temperatures of 900 and 950°C, respectively [S. Mustofa 2019]. This discrepancy in the HRPD results is related by sintering temperatures for both of 58Fe17Cr 25Ni ASS. The two methods also give different calculation results for the lattice parameters. The neutron beam in HRPD has the capability to penetrate deeply in a few cm into the tested material. Therefore, both calculation results are not the same. No other peaks of other phases are found in HRPD patterns, so the austenite phase is considered as the matrix phase of 58Fe17Cr25Ni ASS.

As shown in Fig. 2, Williamson-Hall method can be used to calculate the grain size and micro strains of the two sintering samples from each of the planes in the HRPD patterns. The average diameter of grain sizes formed after sintering at temperature of 900°C is about 142.20 nm and at temperature of 950°C produced about 73.47 nm. As can be seen in Table 2, ASS seems to experience small deformation, so that it is found micro strains about  $4.5373 \times 10^{-4}$  for sintering at a temperature of 900°C and  $7.493 \times 10^{-4}$  for sintering at a temperature of 950°C.

Table 1 Lattice parameters, grain sizes and micro strains of austenite phase measured by HRPD after SPS at 900 and 950°C.

| Sintering temperature (°C) | 900                     | 950                    |
|----------------------------|-------------------------|------------------------|
| Lattice parameter (Å)      | 3.593                   | 3.592                  |
| Grain size (nm)            | 142.20                  | 73.47                  |
| Micro strain               | $4.5373 \times 10^{-4}$ | $7.493 \times 10^{-4}$ |

The microstructure of 58Fe17Cr25Ni ASS sintered at temperature of 900°C is presented in the following Fig. 3. Optical and SEM micrographs clearly show that the microstructure of ASS consists of austenite matrix and particles with small to large size variation spread throughout the matrix. By using an energy-disperse spectrometer, the element content identified in the matrix was 16.82% Cr, 53.06% Fe and 27.08% Ni. The particles, beside of the small Fe and Ni elements, 10.41% and 2.95% respectively, contain a high Cr up to 78.59%. Based on this Cr content, the particles can be considered as  $\alpha'$ -Cr phase. The element mapping in the Fig. 4 confirms that the particles formed contain high Cr. EDS Mapping also shows that the highest Fe and Ni content is found in the matrix of 58Fe17Cr25Ni ASS.

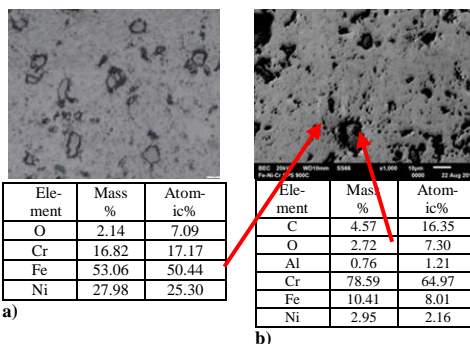
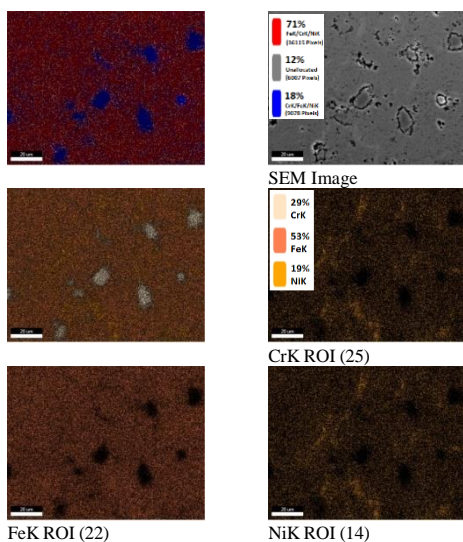
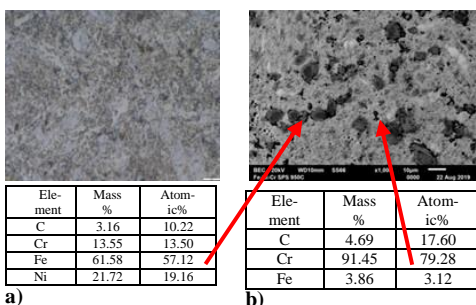


Fig. 3 a) Optical and b) SEM micrographs showing the microstructure and its EDS results of 58Fe17Cr25Ni ASS sintered by SPS at 900°C.



**Fig. 4** SEM micrograph and its element mapping of microstructure of 58Fe17Cr25Ni ASS sintered by SPS at 900°C for 5 minutes.

Optical and SEM micrographs display similar microstructure in the 58Fe17Cr25Ni ASS sintered at temperature of 950°C, as shown in **Fig. 5**. The matrix is dominantly composed of equiaxed austenite grains containing 13.55% Cr, 61.58% Fe and 21.72% Ni while the particles are  $\alpha'$ -Cr containing high Cr up to 91.45% found in the austenite grain boundary. This microstructure formation is also shown by mapping its elements in **Fig. 6**. High Fe and Ni contents are also seen in the matrix containing austenite grains,  $\gamma$ -(Fe,Ni), and a high Cr content is found in the particle of  $\alpha'$ -Cr. The number of particles is estimated to be more in this 58Fe17Cr25Ni ASS. Such a condition is also supported by identifying several light elements, such as C and O, which tend with react to Cr on the matrix and particle surfaces. Therefore, although both the microstructures formed are almost similar, the number of  $\alpha$ -Cr particles appearing on the ASS surface sintered at temperature 950°C tends to be higher as compared on the ASS surface sintered at temperature of 900°C.



**Fig. 5** a) Optical and b) SEM micrographs showing the microstructure and EDS results of 58Fe17Cr25Ni ASS sintered by SPS at 900°C.

The structure of 58Fe17Cr25Ni ASS which sintered at temperature of 900 and 950°C for 5 minutes can be seen in more

detail in the TEM micrograph in **Fig. 7**. In general, the matrix of ASS sintered at 900°C is composed of twin austenite grains (arrow A) at round 600 nm in size and have high density of dislocations (arrow B) as it can be seen in Fig. 7.a.1. Even though it looks unidirectional, slip planes (arrow C) and bands (arrow D) generally appear to be huge deformed within austenite grains as shown in Fig. 7. a. 2. Exceedingly small grains can still be found on some grain boundaries.

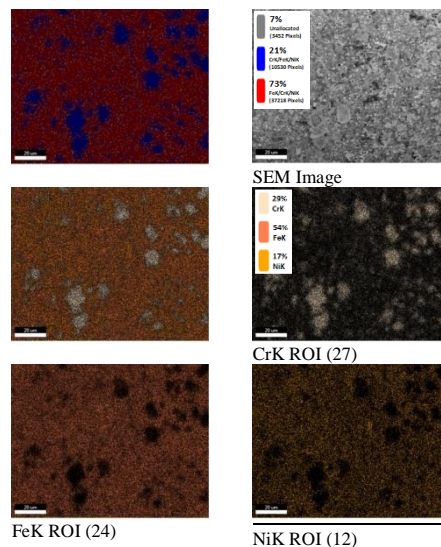


**Fig. 6** SEM micrograph and its element mapping of microstructure of 58Fe17Cr25Ni ASS sintered by SPS at temperature of 950°C for 5 minutes.

Different to the 58Fe17Cr25Ni ASS structure sintered at temperature of 900°C, the structure formed in sintering at temperature of 950°C for 5 minutes as shown in the TEM micrograph in Fig. 7.b1-2, in general, the matrix of 58Fe17Cr25NiASS remains to be composed by twin grain austenite. However, shown in Fig. 7b as its size decreases to be smaller at round 200 nm and known as sub-grains (arrow E). Such a structure mainly nucleates at grain boundaries as a partial recrystallization. Dislocation and slip planes around these sub-grains are still existed to be observed but the amount is estimated much lower than in the 58Fe17Cr25NiASS sintered at 900°C. However, some bubbles (arrow F) formed by trapped air between the particles were still noticed among the austenite grains.

Fig. 7.a.3.-4 shows an austenite grain and a  $\alpha'$ -Cr particle with respectively their electron diffraction pattern in zone axis of  $Zm[111]$  and  $Zp[133]$  obtained from in the 58Fe17Cr25Ni ASS sintered at a temperature of 900°C for time of 5 minutes. Whereas Fig. 7.b.3.-4 shows austenite grains with the electron diffraction patterns in zone axis of  $Zm[013]$  and  $Zm[001]$ , both of which were obtained from the in the matrix of 58Fe17Cr25Ni ASS sintered at temperature of 950°C for time of 5 minutes. Analysis from the electron diffraction patterns of the austenite grains has succeeded to determine that the crystal structure of austenite is a face-centered cubic with a lattice parameter of  $a = 3.5526 \pm 0.0297 \text{ \AA}$ . Moreover, from the electron diffraction patterns obtained that the  $\alpha'$ -Cr particle located between austenite grains, its crystal structure is a body-centered cubic with a lattice parameter  $a = 2.8694 \pm 0.0025 \text{ \AA}$ .

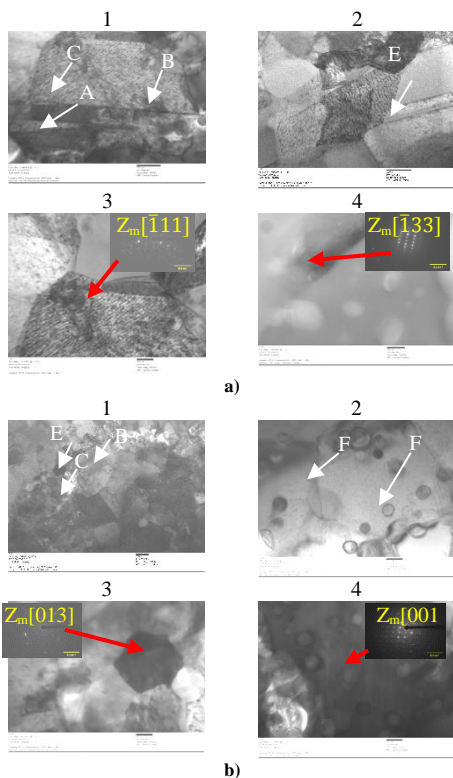


**Fig. 7** TEM images obtained in the 58Fe17Cr25Ni ASS sintered at temperatures of a) 900 and b) 950°C for time of 5 minutes.

#### Alloying 58%Fe, 17%Cr and 25%Ni Powders

Although the alloying reaction occurs under solid conditions, the powders of Fe, Ni and Cr elements during sintering at temperatures of 900 and 950°C can form the equiaxed austenite grains as the matrix of 58Fe17Cr25Ni ASS. The results of the HRPD analysis support the existence of the austenite grains in the ASS with the crystal structure of face-centered cubic and are included in the Fm3m space group. In addition, all Cr mixed in austenite grains cannot be dissolved in solid solutions even though the temperature is set to 950°C so that particles containing high Cr (3.86-10.41% Fe, 78.59-91.45% Cr and 0-2.95% Ni) is found and can be considered as  $\alpha'$ -Cr particles. All processes occurred in a solid state. By contrast, the liquid state dissolved all elements and during solidification, the phase transformation occurs to form the austenite phase which can dissolve maximum about 12%Cr. Because of this solubility limit of austenite phase, the remaining Cr will form a particle. Besides the matrix formed is not yet stable, Cr content exceeds the solubility limit of  $\gamma$ -(Fe, Ni). However, during a solid reaction, increasing the sintering temperature to 950 °C can reduce the amount of Cr content to 13.55% in the matrix of 58Fe17Cr25Ni ASS, approaching the permissible solubility limit for the austenite phase.

The second phase particles which are between the austenite grain boundaries in the ASS have been identified as  $\alpha'$ -Cr particle. Sintering temperature affects the distribution of these particles. The number of particles tends to increase by increas-

ing sintering temperatures from 900°C to 950°C. The high sintering temperature promotes the remaining insoluble Cr in the solid solution of Fe-Ni to accumulate and develop to become the particles of  $\alpha'$ -Cr so that number of particles in the microstructure of ASS sintered at higher temperatures is distributed larger.

As mentioned above, the microstructure of 58Fe17Cr25Ni ASS both sintered at temperature of 900°C and at 950°C for 5 minutes generally consists of austenite grains as matrix and particles of  $\alpha'$ -Cr phase that are spread evenly in the matrix. However, in detail Fig. 7 by looking at TEM micrographs, 58Fe17Cr25Ni ASS formed after sintering at 900°C has twin structure grains with many slip bands, dislocations and sub-grains of austenite between coarse austenite grains. In addition,  $\alpha'$ -Cr particles were observed between the austenite grains. The number of slip bands and dislocations in the grains indicates that the sintering at this temperature has not been able to eliminate defects such as slip bands and dislocations in the austenite grains. Besides that, exceptionally fine grains appear between and within the grains indicating the formation of a sub-structure formed as partial recrystallization.

Different structure as shown in previous structure, although in general 58Fe17Cr25Ni ASS still consists of austenite grains and  $\alpha'$ -Cr particles, micrographs that are more detailed display ultra-fine austenite grains more dominantly. This change is consistent with the HRPD results. The average size of the grains formed is about 73.47 nm, finer and can be said as ultra-fine grains. Although still visible, the slip bands on the ASS are estimated to be exceedingly small. Same likes dislocation defects, it is difficult to observe so it can be said that the density of dislocation decreases with increasing sintering temperature. However, air bubbles appear between the austenite grain boundaries. The air trapped between grain boundaries during the sintering process with the technique of SPS is much decreased. Most air is sucked through the vacuum pump and a small portion is trapped in between powder particles, forming air bubbles and does not reduce ASS hardness as stated in the previous paper [S. Mustofa 2019]. The high hardness of sintered ASS is more due to the high density of ASS as mentioned in previous paper.

#### CONCLUSIONS

Based on the discussion of microstructure including its detail formation in the 58Fe17Cr25Ni ASS formed from powders of 58%Fe, 17%Cr and 25%Ni sintered at temperatures of 900 and 950°C and hold for 5 minutes, it can be drawn some conclusion as followed:

- The microstructure of 58Fe17Cr25Ni ASS sintered at temperatures of 900 and 950°C have matrix of equiaxed austenite grains which structured face-centered cubic (FCC) and particles with high Cr content,  $\alpha'$ -Cr, which structured body-centered cubic, spread in the whole matrix.
- Increasing sintering temperature increase the number of  $\alpha'$ -Cr particles appear in the 58Fe17Cr25Ni ASS.
- Most austenite grains still contain of a lot of slip bands and dislocation even sintered a temperature of 900°C for 5 minutes.
- Although, some defects are noticed in the austenite grains, most regions of grains experience recovery and partial recrystallization after sintering the 58Fe17Cr25Ni ASS at temperature of 950°C for 5 minutes.

**Acknowledgments:** The authors would like to express their appreciation for excellent support and coordinator so that this research can be finished properly to the Head of the Center for

Science and Technology for Advanced Materials and Head of BTBM, Dr. Iwan Sumirat, and Head of PSTBM, Dr. Abu Khalid Rivai. This research was supported by Insinas Project No.06/INS-1/PPK/E4/2019.

## REFERENCES

1. C. Keller, K. Tabaiaiev, G. Marnier, J. Noudem, X. Sauvage, E. Hug: *Materials Science & Engineering A*, 665, 2016, 125-134. <https://doi.org/10.1016/j.msea.2016.04.039>.
2. F. Akhtar, L. Ali, F. Peizhong, J. Ali Shah: *Journal of Alloys and Compounds*, 509(35), 2011, 8794-8797. <https://doi.org/10.1016/j.jallcom.2011.06.077>.
3. I. Vlčková, P. Jonšta, Z. Jonšta, P. Váňová, T. Kulová: *Metals*, 6(12), 2016, 319. <https://doi.org/10.3390/met6120319>.
4. J. P. Choi et al.: *Powder Technology*, 279, 2015, 196-202. <https://doi.org/10.1016/j.powtec.2015.04.014>.
5. K. J. Ducki: *Analysis of the Precipitation and Growth Processes of the Intermetallic Phases in an Fe-Ni Superalloy*, Ed. Mahmood Aliofkhaezrai, 2015. <https://dx.doi.org/10.5772/61159>.
6. K. Sakata, *ISIJ International*, 46(12) 2006, 1795-1799. <https://doi.org/10.2355/isijinternational.46.1795>.
7. M. Dani, S. Mustofa, Parikin, Sumaryo, T. Sudiro, B. Hermanto, D. R. Adhika, A. Insani, A. Dimiyati, Syahbuddin, S. Hardjanto, E. A. Basuki, C. A. Huang: Effect of Spark Plasma Sintering (SPS) at Temperatures of 900 and 950°C for 5 minutes on Microstructural Formation of Fe-25Ni-17Cr Austenitic Stainless Steel, *The 6<sup>th</sup> International Conference on Engineering, Technology, and Industrial Application (ICETIA)*, 11-12 Dec 2019, University of Muhammadiyah Surakarta, Alila Hotel, Solo, Laweyan, Indonesia.
8. M. McGuire, *Stainless Steel for Design Engineers*, ASM International, Ohio, USA, 2008.
9. P. Cavaliere (Editor): *Spark Plasma Sintering of Materials: Advances in Processing and Applications*, Springer, 2019. <https://doi.org/10.1007/978-3-030-05327-7>.
10. R. L. Plaut, C. Herrera, D. M. Escriba, P. R. Rios, A. F. Padilha: *Materials Research*, 10(4), 2007, 453-460. <https://doi.org/10.1590/S1516-14392007000400021>.
11. S. Mustofa, M. Dani, Parikin, T. Sudiro, B. Hermanto, D. R. Adhika, Syahbuddin, C. A. Huang: Effect of Temperature of Spark Plasma Sintering on the Development of Oxide Compound in Fe-25wt%Ni-17wt%Cr Austenitic Stainless Steel, *The 6<sup>th</sup> International Conference on Engineering, Technology, and Industrial Application*, 11-12 Dec 2019, University of Muhammadiyah Surakarta, Alila Hotel Solo, Laweyan, Indonesia.
12. S. J. Zinkle, J. T. Busby: *Materials Today*, 12(11) 2009, 12-19. [https://doi.org/10.1016/S1369-7021\(09\)70294-9](https://doi.org/10.1016/S1369-7021(09)70294-9).
13. T. Sourmail: *Materials Science and Technology*, 17(1) 2001, 1-14. <https://doi.org/10.1179/026708301101508972>.